Available online at www.sciencedirect.com

ScienceDirect

Mendeleev Commun., 2021, **31**, 872–874

Mendeleev Communications

Promotion of cobalt catalyst for Fischer–Tropsch synthesis by molybdenum as protection against sulfur poisoning

Tshepo D. Dipheko,[a,b,c] Oleg L. Eliseev,*[a] Yurii A. Agafonov,[a] Maria V. Tsapkina,[a] Vladimir V. Maximov,[a] Mohamed E. Osman,[a,b] Alexander G. Cherednichenko[b] and Victor M. Kogan[a]

[a] *N. D. Zelinsky Institute of Organic Chemistry, Russian Academy of Sciences, 119991 Moscow, Russian Federation. E-mail: oleg@ioc.ac.ru*

[b] *Peoples Friendship University of Russia (RUDN University), 117198 Moscow, Russian Federation*

[c] *Material Science Innovation and Modelling (MaSIM) Research Focus Area, Faculty of Natural and Agricultural Sciences, North-West University (Mafikeng Campus), Mmabatho 2735, South Africa*

DOI: 10.1016/j.mencom.2021.11.035

Molybdenum promotion was used to increase the resistance of a cobalt catalyst for the Fischer–Tropsch synthesis to sulfur poisoning. A series of experiments on adding 1,3,5-trithiane to synthesis gas (sulfur content of 1 ppm) showed that the Co–Mo/Al_2O_3 catalyst regained its initial activity after 8 h of operation. In comparison, catalysts not containing molybdenum experienced a significant irreversible loss of activity that was not recovered after stopping the addition of 1,3,5-trithiane to the feed.

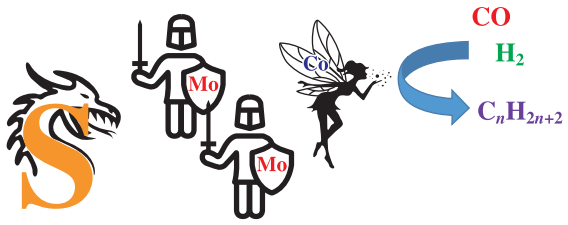

Keywords: Fischer–Tropsch synthesis, cobalt catalyst, molybdenum, sulfur, poisoning.

The production of higher hydrocarbons from CO and H_2 (Fischer–Tropsch synthesis) is one of the most developed alternative methods for producing components of motor fuels, base oils, wax and other chemical products from non-petroleum feedstocks. Unlike petroleum fractions, synthetic hydrocarbons do not contain nitrogen and sulfur compounds, polyaromatic compounds and heavy metals.[1–3] Since the environmental purity of products is one of the priority areas of modern basic organic synthesis, synthetic hydrocarbons production is becoming especially relevant.

An immense advantage of the Fischer–Tropsch process is its broad and practically unlimited feedstock base: synthesis gas can be obtained from various carbon-containing sources, including natural and associated gases, heavy oil residues, coal and biomass.[4–7] It is important to note that the use of renewable raw materials such as biomass for the production of synthesis gas significantly reduces the carbon footprint of the entire process chain and thereby contributes to the control of anthropogenic greenhouse gas emissions and global warming.[8]

Synthesis gas obtained by gasification of heavy feedstock (coal, petroleum coke and biomass) contains numerous impurities of volatile sulfur, nitrogen and halogen compounds. To one degree or another, all of them are poisonous to cobalt and iron catalysts for the Fischer–Tropsch synthesis and, therefore, must be removed from the gas. The desired level of purification varies according to different sources, although it is generally very high – the content of sulfur compounds should not exceed hundredths of ppm, nitrogen 0.01–10 ppm and halides 0.01 ppm.[7–10]

It should be noted that cobalt catalysts for the Fischer–Tropsch synthesis are much more expensive than their iron counterparts, and their nominal operating life before replacement is one year or more.[11] Therefore, the issue of cobalt catalysts poisoning with impurities in the feedstock remains urgent. The solution could be to create catalyst compositions that are less sensitive to poisoning impurities, particularly S-containing, than modern cobalt catalysts.

Molybdenum oxide is a key component of catalysts for the hydrotreating of petroleum fractions[12–14] and the synthesis of higher alcohols from CO and H_2.[13,14] Well-known cobalt– and nickel–molybdenum-sulfide catalysts in the active state contain molybdenum sulfide, MoS_2, which is formed by the preliminary sulfidation of the oxide precursor, as well as during the interaction of the catalyst surface with sulfur-containing impurities of the feed. The idea is to promote a cobalt catalyst for the synthesis of hydrocarbons with molybdenum, which, in the case of the presence of sulfur compounds in the synthesis gas, will play the role of a 'sulfur protector' reversibly chemisorbing sulfur-containing impurities in the synthesis gas and thereby protecting cobalt from poisoning:

$$MoO_2 + 2H_2S \rightleftharpoons MoS_2 + 2H_2O. \quad (1)$$

Note that earlier, the promotion of cobalt catalyst for the Fischer–Tropsch synthesis with molybdenum was described in the only article[15] in which the protective effect of molybdenum against sulfur poisoning was not examined.

H_2S is commonly used as the sulfur source, while other substances such as dimethyl sulfide,[16] COS,[17,18] CS_2[19] and SO_2[20] are also mentioned in the literature. The complexity of experiments associated with the use of such toxic gases or volatile liquids prompted us to use 1,3,5-trithiane as a model S-carrier substance. It is an easy-to-handle solid which can be accurately dosed.

To study the protective effect of molybdenum on a cobalt catalyst for the synthesis of hydrocarbons, we prepared an impregnated Co–Mo/Al_2O_3 catalyst containing 20% cobalt and 5% molybdenum. The Co/Al_2O_3 catalyst, which is similar in

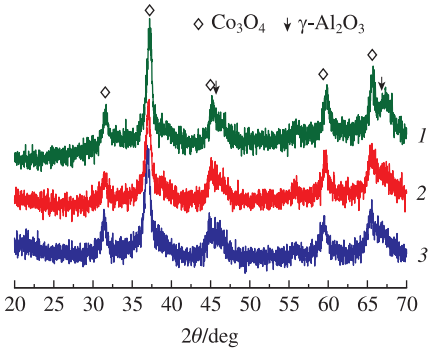

Figure 1 X-ray diffraction patterns of cobalt catalysts for the Fischer–Tropsch synthesis: (*1*) Co–Re–Pd/Al_2O_3, (*2*) Co/Al_2O_3 and (*3*) Co–Mo/Al_2O_3.

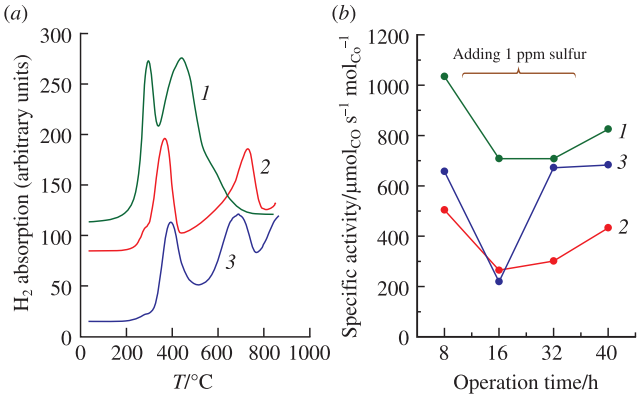

Figure 2 (*a*) TPR curves and (*b*) the effect of sulfur poisoning on the specific activity of cobalt catalysts for the Fischer–Tropsch synthesis: (*1*) Co–Re–Pd/Al_2O_3, (*2*) Co/Al_2O_3 and (*3*) Co–Mo/Al_2O_3.

composition but does not contain a molybdenum promoter, and the Co–Re–Pd/Al_2O_3 catalyst promoted with noble metals, which previously showed high activity in the synthesis of hydrocarbons from CO and H_2, were used as reference samples.†

In X-ray diffraction patterns (Figure 1), the calcined catalysts showed reflexes at 45.7 and 66.5°, corresponding to γ-Al_2O_3, and peaks at 2θ values of 31.5, 36.9, 44.9, 59.5 and 65.5°, which should be attributed to the Co_3O_4 spinel.[22,23] The rest of the catalyst components were not displayed on X-ray images, apparently due to their high dispersion. The average size of the Co_3O_4 crystals was calculated from the broadening of the (311) peak at 2θ = 36.9° using the Scherrer equation.[24] It was 12.2 nm for Co/Al_2O_3, 12.9 nm for Co–Mo/Al_2O_3 and 12.4 nm for Co–Re–Pd/Al_2O_3. Therefore, the dispersion of cobalt in all three catalysts is virtually the same.

Hydrogen absorption profiles of the catalysts in TPR experiments are shown in Figure 2(*a*). Several absorption peaks correspond to a stepwise Co_3O_4 reduction process. This oxide is formed during the thermal decomposition of Co^{II} nitrate upon calcination and is reduced in two stages:[22]

$$Co_3O_4 + H_2 \longrightarrow 3CoO + H_2O, \quad (2)$$

$$CoO + H_2 \longrightarrow Co + H_2O. \quad (3)$$

The first reduction stage proceeds in the Co/Al_2O_3 and Co–Mo/Al_2O_3 samples with the maximum hydrogen absorption at 370–390 °C. The next absorption peak with a maximum at 690–720 °C corresponds to the reduction of CoO to metal. The significant peak width is probably associated with the polydispersity of the reduced phase and its various interaction modes with the support, up to the formation of mixed Co–Al oxides.[22,25] In addition, at high temperatures in the Co–Mo/Al_2O_3 sample, there is a stepwise reduction of sputtered MoO_3 and, probably, mixed $CoMoO_4$ oxides.[15]

The TPR curve [see Figure 2(*a*), curve *1*] of Co–Re–Pd/Al_2O_3 differs markedly from those for other catalysts by a significant shift of both absorption peaks to the low-temperature region. In addition, the reduction of this catalyst is practically completed at 800 °C, which is not the case for Co/Al_2O_3 and Co–Mo/Al_2O_3. Pd and Re in the catalyst composition probably contribute to the reduction of Co_3O_4. The effect of noble metal additives on the reducibility of cobalt catalysts is well known.[26] Rhenium also promotes the reduction, albeit to a lesser extent and, apparently, only at the stage of CoO reduction to metallic Co.[25–27]

Investigation of the surface of the original Co–Mo/Al_2O_3 sample by X-ray microanalysis [Figures 3(*a*),(*b*)] showed a uniform distribution of cobalt and molybdenum over the catalyst. Thus, both metals are in close contact with each other, and molybdenum can mainly act as a 'sulfur protector' for the adjacent metallic cobalt phase.

† The Co/Al_2O_3 and Co–Re–Pd/Al_2O_3 catalysts were prepared by incipient wetness impregnation of γ-Al_2O_3 (S_{sp} = 219 m^2 g^{-1}, V_{sp} = 0.74 cm^3 g^{-1}) with aqueous solutions of $Co(NO_3)_2{\cdot}6H_2O$, NH_4ReO_4 and $PdCl_2$, respectively. The precursor salts were taken in amounts to ensure that the catalysts contained Co (20 wt%), Re (0.5 wt%) and Pd (0.1 wt%). The impregnated materials were dried on a water bath at 60–80 °C and then calcined in the air flow at 400 °C for 3 h. The Co–Mo/Al_2O_3 catalyst was prepared by applying 5% Mo from an aqueous $(NH_4)_6Mo_7O_{24}{\cdot}4H_2O$ solution to the previously obtained Co/Al_2O_3, followed by calcination as indicated above.

The catalysts were investigated by temperature-programmed reduction (TPR) using a chromatographic type instrument. A catalyst sample (50 mg) was placed in a quartz flow reactor, purged with dried He at 300 °C for 2 h and then cooled to 50 °C in the He flow. For recording the hydrogen absorption curves, the reactor was heated to 850 °C at a rate of 20 °C min^{-1} in a mixture flow of H_2 (10.0 vol%) and Ar (90.0 vol%).

Sample microstructure was investigated by field emission scanning electron microscopy on a Hitachi SU-8000 electron microscope. Analytical measurements have been optimized using the previously described approach.[21] Before imaging, the sample was placed on the surface of an aluminum stage 25 mm in diameter, fixed with conductive plasticine, and a conductive carbon layer 10 nm thick was sputtered on it. Images were obtained in the secondary electron registration mode at an accelerating voltage of 10 kV. Sample morphology was studied, taking into account the correction for the surface effects of the conductive layer sputter. The sample was examined by X-ray microanalysis on a Hitachi SU-8000 electron microscope using an Oxford Instruments X-max 80 energy dispersive X-ray spectrometer at an accelerating voltage of 20 kV.

Catalytic tests were carried out in a flow-through device with a steel tube reactor heated by an electric furnace. A 400 mg catalyst sample was diluted with 10 cm^3 of silica sand to prevent local overheating and placed in the isothermal zone of the reactor with an inserted thermocouple. The catalyst was activated immediately before testing by passing H_2 at a flow rate of 2 Ndm^3 h^{-1} and a temperature of 400 °C for 4 h. After activation, synthesis gas containing CO (34 vol%), H_2 (60 vol%) and Ar (6 vol%) was fed into the cooled reactor; the pressure in the reactor was set at 2 MPa. The synthesis gas flow rate was maintained at 2±0.05 Ndm^3 h^{-1}. The temperature was increased stepwise from 180 to 210 °C in 10 °C steps; the duration of operation at each temperature step was 8 h. Further, the catalysts were tested at 210 °C for resistance to sulfur poisoning.

A solution of 1,3,5-trithiane in ethanol was fed into the reactor using a microdosing device so that the mole fraction of sulfur in synthesis gas was 1 ppm. The total amount of the injected solution did not exceed 4 cm^3. Therefore, ethanol in the reaction zone could not significantly affect the performance of the catalyst. After 16 h of operation with sulfurized synthesis gas, 1,3,5-trithiane feeding was stopped, so the synthesis gas became free of sulfur.

Gaseous synthesis products were analyzed by gas adsorption chromatography on LCM-80 instruments equipped with columns (1 m ×3 mm) packed with 5A molecular sieves (CH_4 and CO) and Porapak Q (C_2, C_3, C_4 and CO_2) using helium as carrier gas and a katharometer type detector. CO conversion and selectivity to carbon-containing synthesis products were calculated from chromatographic data. The specific activity of the samples was calculated by relating the CO conversion rate to the cobalt mass in the catalyst.

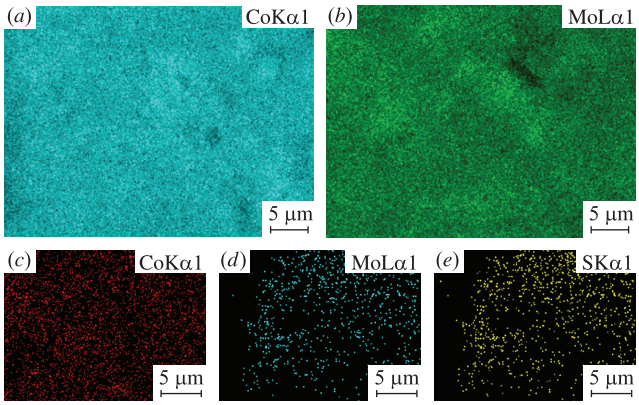

Figure 3 Distribution of (*a*),(*c*) cobalt, (*b*),(*d*) molybdenum and (*e*) sulfur in the (*a*),(*b*) original and (*c*)–(*e*) spent Co–Mo/Al_2O_3 catalyst according to the data of X-ray microanalysis.

The tests of this catalyst in the low-temperature Fischer–Tropsch synthesis were carried out after its activation with hydrogen and pretreatment in a synthesis gas flow with a gradual increase in temperature to 210 °C. The CO conversion was 12.9% at this temperature, with a selectivity of 79.5% to liquid hydrocarbons and 5.6% to methane. Then, an ethanol solution of 1,3,5-trithiane was fed to the reactor along with synthesis gas to ensure that the volumetric sulfur content of the synthesis gas was one part per million (1 ppm). In the first hours of operation with such a feedstock, the activity decreased by three times, while selectivities to methane and lower hydrocarbons (C_2–C_4), on the contrary, increased significantly. A sharp increase in CO_2 selectivity was also noted. No doubt, the change in the synthesis parameters was caused by sulfur poisoning of the catalyst. However, after 16 h of operation, the activity of the catalyst increased again and even slightly exceeded the initial level – the CO conversion was 13.2%. Selectivities to CH_4 and CO_2 decreased, while selectivities to gaseous C_2–C_4 hydrocarbons remained high. After the cessation of 1,3,5-trithiane feed, the catalyst activity remained at the same level, and the selectivity values almost returned to the initial values, although the selectivity to the target liquid hydrocarbons (C_{5+}) decreased slightly compared to the initial value (Table 1).

Reference catalysts, *viz.* Co/Al_2O_3 and Co–Re–Pd/Al_2O_3, were tested similarly. Figure 2(*b*) shows the change in the specific activity of catalysts when adding 1,3,5-trithiane to the feed. Unlike Co–Mo/Al_2O_3, which regained its initial activity after eight hours of supplying sulfur-containing synthesis gas, both reference catalysts lost up to half of their original activity. Moreover, these samples did not fully recover their activity after stopping the supply of 1,3,5-trithiane to the synthesis gas. X-ray microanalysis of the spent Co–Mo/Al_2O_3 sample showed that the localization of sulfur on the surface coincides with the localization of molybdenum, not cobalt, which confirms our assumption about the protective function of the molybdenum promoter [Figures 3(*c*)–(*e*)].

We interpret the obtained data as the result of the protection of metallic cobalt (an active phase in the synthesis of hydrocarbons) with molybdenum from sulfur poisoning. The catalyst contains molybdenum as oxide MoO_2, capable of absorbing sulfur supplied with the feedstock and turning it into sulfide MoS_2. In addition, it is likely that sulfur initially adsorbed on cobalt is also transferred to molybdenum with the formation of sulfide MoS_2. This interpretation can explain the recovery of catalytic activity after initial deactivation during operation with synthesis gas containing sulfur.

As a result, the introduction of molybdenum oxide into the catalyst formulation increases its resistance to sulfur poisoning. After stopping the supply of sulfur-contaminated synthesis gas, the catalytic activity is completely restored, and the selectivity to the target liquid hydrocarbons reaches 94% of the initial level.

Table 1 Test results of the Co–Mo/Al_2O_3 catalyst in the synthesis of hydrocarbons from CO and H_2 at T = 210 °C.

Operation time/h	Sulfur/ppm	CO conversion (%)	Selectivity (mol%)			
			CH_4	C_2–C_4	C_{5+}	CO_2
8	0	12.9	5.6	14.2	79.5	0.7
16	1	4.3	19.0	32.4	46.7	1.9
24	1	13.2	1.3	39.5	58.7	0.5
40	0	13.4	8.5	15.7	75.1	0.7

This work was supported by the Russian Foundation for Basic Research (grant no. 19-53-60002). The authors are grateful to the Department of Structural Research, ZIOC RAS for electron microscopy studies and to Prof. I. V. Mishin for X-ray diffraction analysis.

References

1 A. L. Lapidus, *Bull. Acad. Sci. USSR, Div. Chem. Sci.*, 1991, **40**, 2335 (*Izv. Akad. Nauk SSSR, Ser. Khim.*, 1991, 2681).
2 A. A. Adesina, *Appl. Catal., A*, 1996, **138**, 345.
3 M. E. Dry, *Appl. Catal., A*, 2004, **276**, 1.
4 H. Boerrigter and R. Rauch, in *Handbook Biomass Gasification*, ed. H. A. M. Knoef, BTG Biomass Technology Group, Enschede, The Netherlands, 2005, pp. 221–230.
5 K. Aasberg-Petersen, I. Dybkjær, C. V. Ovesen, N. C. Schjødt, J. Sehested and S. G. Thomsen, *J. Nat. Gas Sci. Eng.*, 2011, **3**, 423.
6 I. V. Zagaynov, A. S. Loktev, I. E. Mukhin, A. A. Konovalov, A. G. Dedov and I. I. Moiseev, *Mendeleev Commun.*, 2019, **29**, 22.
7 D. Chiche, C. Diverchy, A.-C. Lucquin, F. Porcheron and F. Defoort, *Oil Gas Sci. Technol.*, 2013, **68**, 707.
8 H. Jahangiri, J. Bennett, P. Mahjoubi, K. Wilson and S. Gu, *Catal. Sci. Technol.*, 2014, **4**, 2210.
9 M. J. A. Tijmensen, A. P. C. Faaij, C. N. Hamelinck and M. R. M. van Hardeveld, *Biomass Bioenergy*, 2002, **23**, 129.
10 H. Boerrigter, H. den Uil and H.-P. Calis, in *Pyrolysis and Gasification of Biomass and Waste*, ed. A. V. Bridgwater, CPL Press, Newbury, UK, 2003, pp. 371–383.
11 G. Schaub, M. Rohde and A. Mena Subiranas, in *Proceedings of the DGMK/SCI-Conference 'Synthesis Gas Chemistry'*, DGMK, Hamburg, 2006, pp. 75–84.
12 J. S. Lee and M. Boudart, *Appl. Catal.*, 1985, **19**, 207.
13 V. M. Kogan, P. A. Nikul'shin, V. S. Dorokhov, E. A. Permyakov, A. V. Mozhaev, D. I. Ishutenko, O. L. Eliseev, N. N. Rozhdestvenskaya and A. L. Lapidus, *Russ. Chem. Bull., Int. Ed.*, 2014, **63**, 332 (*Izv. Akad. Nauk, Ser. Khim.*, 2014, 332).
14 V. S. Dorokhov, D. I. Ishutenko, P. A. Nikul'shin, O. L. Eliseev, N. N. Rozhdestvenskaya, V. M. Kogan and A. L. Lapidus, *Dokl. Chem.*, 2013, **451**, 191 (*Dokl. Akad. Nauk*, 2013, **451**, 291).
15 C. G. Cooper, T.-H. Nguyen, Y.-J. Lee, K. M. Hardiman, T. Safinski, F. P. Lucien and A. A. Adesina, *Catal. Today*, 2008, **131**, 255.
16 S. S. Pansare and J. D. Allison, *Appl. Catal., A*, 2010, **387**, 224.
17 Z.-T. Liu, J.-L. Zhou and B.-J. Zhang, *J. Mol. Catal.*, 1994, **94**, 255.
18 Z.-T. Liu, Y.-W. Li, J.-L. Zhou, Z.-X. Zhang and B.-J. Zhang, *Appl. Catal., A*, 1997, **161**, 137.
19 R. J. Madon and H. Seaw, *Catal. Rev.: Sci. Eng.*, 1977, **15**, 69.
20 M. Wolf, C. Schüler and O. Hinrichsen, *J. CO_2 Util.*, 2019, **32**, 80.
21 V. V. Kachala, L. L. Hemchyan, A. S. Kashin, N. V. Orlov, A. A. Grachev, S. S. Zalesskiy and V. P. Ananikov, *Russ. Chem. Rev.*, 2013, **82**, 648.
22 Ø. Borg, S. Eri, E. A. Blekkan, S. Storsæter, H. Wigum, E. Rytter and A. Holmen, *J. Catal.*, 2007, **248**, 89.
23 Z. Cai, J. Li, K. Liew and J. Hu, *J. Mol. Catal. A: Chem.*, 2010, **330**, 10.
24 B. D. Cullity and S. R. Stock, *Elements of X-Ray Diffraction*, 3rd edn., Pearson, Upper Saddle River, NJ, 2001.
25 G. Jacobs, T. K. Das, Y. Zhang, J. Li, G. Racoillet and B. H. Davis, *Appl. Catal., A*, 2002, **233**, 263.
26 A. Y. Khodakov, W. Chu and P. Fongarland, *Chem. Rev.*, 2007, **107**, 1692.
27 A. M. Hilmen, D. Schanke and A. Holmen, *Catal. Lett.*, 1996, **38**, 143.

Received: 10th June 2021; Com. 21/6584